# REPORT DOCUMENTATION PAGE

Form Approved
OMB No. 0704-0188



| 1. REPORT DATE *(DD-MM-YYYY)* | 2. REPORT TYPE | 3. DATES COVERED *(From - To)* |
|---|---|---|
| | Technical Papers | |

**4. TITLE AND SUBTITLE**

**5a. CONTRACT NUMBER** N/A

**5b. GRANT NUMBER**

**5c. PROGRAM ELEMENT NUMBER**

**6. AUTHOR(S)**

**5d. PROJECT NUMBER** 2308

**5e. TASK NUMBER** M19B

**5f. WORK UNIT NUMBER**

**7. PERFORMING ORGANIZATION NAME(S) AND ADDRESS(ES)**

Air Force Research Laboratory (AFMC)
AFRL/PRS
5 Pollux Drive
Edwards AFB CA 93524-7048

**8. PERFORMING ORGANIZATION REPORT**

**9. SPONSORING / MONITORING AGENCY NAME(S) AND ADDRESS(ES)**

Air Force Research Laboratory (AFMC)
AFRL/PRS
5 Pollux Drive
Edwards AFB CA 93524-7048

**10. SPONSOR/MONITOR'S ACRONYM(S)**

**11. SPONSOR/MONITOR'S NUMBER(S)**

**12. DISTRIBUTION / AVAILABILITY STATEMENT**

Approved for public release; distribution unlimited.

**13. SUPPLEMENTARY NOTES**

**14. ABSTRACT**

**15. SUBJECT TERMS**

| 16. SECURITY CLASSIFICATION OF: | | | 17. LIMITATION OF ABSTRACT | 18. NUMBER OF PAGES | 19a. NAME OF RESPONSIBLE PERSON |
|---|---|---|---|---|---|
| a. REPORT | b. ABSTRACT | c. THIS PAGE | | | Leilani Richardson |
| Unclassified | Unclassified | Unclassified | A | | 19b. TELEPHONE NUMBER *(include area code)* (661) 275-5015 |



21 separate items enclosed

103 041

J308P119B

TP-FY99-0141 9B

✓Spreadsheet
✓DTS

MEMORANDUM FOR PRS (Contractor/In-House Publication)

14 June 1999

FROM: PROI (TI) (STINFO)

SUBJECT: Authorization for Release of Technical Information, Control Number: AFRL-PR-ED-TP-FY99-0141
Young, Muntz and Ketsdever , "Unique Hollow Cathode as a Candidate Non-Magnetic Ion Thruster"
**AIAA** **(Public Release)**

# Unique Hollow Cathode as a Candidate Non-Magnetic Ion Thruster

Marc Young† and E.P. Muntz*
University of Southern California
Department of Aerospace Engineering
Los Angeles, California

and

Andrew D. Ketsdever§
Air Force Research Laboratory
Propulsion Directorate
Edwards AFB, California



## Abstract

The applicability of a unique discharge chamber, previously studied by VI Miljevic, as the ion source for a meso-scale ion thruster was investigated. The discharge chamber geometry was chosen due to promising reported results which appeared to alleviate the requirement of external magnetic fields while achieving an adequate degree of ionization. The earlier results from spectroscopic studies on the discharge chamber indicated a high degree of ionization, making it a candidate configuration for an ion thruster. An estimate of the degree of ionization using a simple model of the discharge indicated a low achievable ionization, which stimulated further examination of Miljevic's work. The previous spectroscopic studies were repeated and discrepancies were found. Additional spectroscopic and Langmuir probe measurements were made in the plume to determine the degree of ionization of the discharge chamber for several operating conditions. The degree of ionization was experimentally shown to be 0.06-0.15%. A simple extraction ring increases the degree of ionization by roughly a factor of 3.

---

† Research Assistant, Student Member
* A.B. Freeman Professor, Fellow
§ Senior Research Engineer, Senior Member

# I. Introduction

## A.) Ion Thruster Scaling Issues

The current trend towards smaller spacecraft produces a corresponding requirement for smaller thrusters. Magnetic fields place a lower bound on the size to which traditional ion thrusters can be scaled.[1] Full scale ion thrusters use magnetic fields to increase electron path lengths and thus provide the necessary levels of ionization. The spiraling electrons must have a gyroradius small enough to keep them from striking the walls of the discharge chamber. Since gyroradii scale inversely with magnetic field strength, smaller discharge chambers require larger magnetic fields. A practical limit on the magnetic field that can be applied to the thruster creates a limit to the smallest size a discharge chamber can be scaled. Another method of providing adequate degrees of ionization needs to be found for micro ion thrusters.

One possible solution is to enhance the discharge chamber geometry to provide the required degree of ionization. If this is accomplished for a given size of thruster, then by following simple scaling parameters the thruster can be scaled to different sizes. The small size and relative simplicity of this type of thruster would lend itself to being arrayed in relatively large groups of thrusters in order to provide scalability. There are many different quantities that can be affected when scaling an electric discharge, including the electric field, breakdown potential, current density, space charge density, and drift velocity. Scaling properties for simple planar electrodes have been extensively studied and are well understood.[2] There are three quantities that must be matched if planar electrode discharges are to be similar. These are pd, E/p and $J/p^2$ where p is the gas pressure, d is the characteristic dimension, E is the electric field, and J is the current density. The pd product determines the breakdown characteristics of the discharge chamber according to Paschen's law as shown in Eq. 1. This quantity is a measure of the number of collisions that a particle undergoes during its travel through the discharge chamber. The breakdown potential is

$$V_{BK} = \frac{Bpd}{\ln\left(\frac{Apd}{\ln(1+1/\gamma)}\right)} \tag{1}$$

The E/P quantity determines the energy gained by a charged particle between collisions. The current density varies with $p^2$ which provides the Townsend similarity relation that for pd and $J/p^2$ scaling the discharges will have similar breakdown and electrical characteristics. Much less is known about the scaling of other types of discharges.

## B.) Requirements for ion microthrusters

There are certain operational capabilities that must be met by a discharge chamber if it is to be used in a small scale ion thruster. By assuming that the Non-Magnetic Ion Micro-Thruster (NMIMT) should have similar specific power levels for a given $I_{sp}$, the necessary degree of ionization for the small scale discharge chamber can be estimated. This is reasonable since the required velocity increment for spacecraft does not depend on the spacecraft size. Table 1 shows characteristics of typical full scale ion thrusters.

| | Specific Impulse (s) | Thrust (mN) | Size (cm) | Specific Power (W/mN) |
|---|---|---|---|---|
| ETS-VI IES ion engine | 3000 | 20 | 12 | 37 |
| NSTAR | 3310 | 92 | 30 | 25 |
| XIPS-13 | 2585<br>2720 | 17.8<br>18 | 13 | 23 |
| RIT-10 RF ion engine | 3000<br>3150 | 15 | 10 | 39 |

Table 1: Representative Characteristics of a Sample of Full Scale Ion Thrusters[3]

The total $I_{sp}$ for any electric thruster is the sum of the neutral ($I_{sp,n}$) and ion components ($I_{sp,I}$) given by

$$I_{sp} = \{(1-\alpha_I) I_{sp,n} + I_{sp,I}\alpha_I\} \tag{2}$$

where $\alpha_I$ is the degree of ionization in the thruster. The specific impulse of the ion and neutral components are given by

$$I_{sp,I} = \frac{V_{ex}}{g_o} \qquad V_{ex,I} = \left\{\frac{2(1.602x10^{-19}\Delta V}{(1.67x10^{-27})(mw)}\right\}^{\frac{1}{2}} \tag{3}$$

$$I_{sp,N} = \frac{\left(\frac{2(\gamma+1)}{\gamma}\frac{kT_o}{m}\right)^{\frac{1}{2}}}{g_o} \tag{4}$$

where $\gamma$ is the ratio of the specific heats, k is Boltzmann's constant, $T_o$ is the temperature of the propellant gas, $g_o$ is standard gravity, m is the molecular mass of the propellant gas, $V_{ex}$ is the exit velocity of the gas, $\Delta V$ is the accelerating voltage applied to the ions, and mw is the molecular weight of the propellant gas. The applied power per unit thrust is then given by Eq 5.

$$\frac{P_T}{Th_T} = \frac{P_D + \frac{1}{2}\alpha_I \dot{m}(I_{sp,I} g_o)^2}{(1-\alpha_I) I_{sp,N} \dot{m} g_o + I_{sp,I}\alpha_I \dot{m} g_o} \tag{5}$$

where $P_D$ is the discharge power of the thruster and $\dot{m}$ is the mass flow of the propellant gas through the thruster. Fig. 1 shows the effect of degree of ionization on the specific power and specific impulse for the initial discharge chamber chosen for the NMIMT. The exit diameter for the thruster was 1 mm. A typical acceleration voltage of 1000 V was assumed. The gas temperature was assumed to be 1000K with the discharge voltage and current of 500V and 10 mA, respectively.

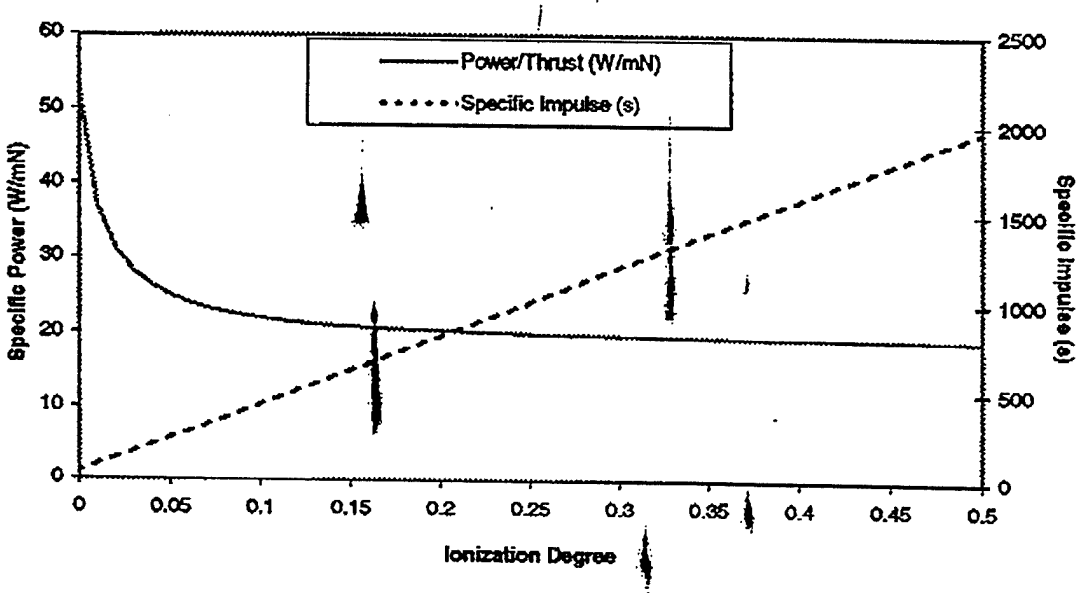


Fig. 1 Effect of ionization degree on performance of a NMIMT

### C.) NMIMT discharge chamber concept

For over ~~fifty~~ 50 years, hollow anode plasma sources have been used in a wide variety of applications including electron beam welding, material processing, and lasers.[4,5,6] Recently, hollow anode plasma sources which utilize gas dynamic ring jets have been used in an attempt to increase the degree of ionization near the exit aperture of the anode.[7,8,9] In this configuration, the hollow anode devices resemble typical large scale (~30 cm) ion thrusters which utilize magnetic field confinement of the electrons and ion accelerating grids. In reviewing the literature on hollow anode discharges, the work of Miljevic[10,11,12,13] appeared to be quite interesting from a micropropulsion standpoint. Miljevic used a 5-mm hemispherical cathode with a 1-mm orifice which acted as the hollow anode. The voltage-current characteristics for this device appear quite attractive for overall power usage[12] and results showed that no electrode material was seen in spectra taken near the exit plane of the thruster indicating little or no degredation.[13] The most intriguing result was that no neutral lines were detected in spectra taken over a wide range of wavelengths (220 – 900 nm) implying a rather high degree of ionization in an argon discharge. It appeared worthwhile to pursue this device as a potential ion source for a micropropulsion system since the high degree of ionization was obtained without the use of magnetic containment of the electrons.

The discharge chamber shown in Fig. 2 has a 5-mm radius hemispherical, aluminum cathode. A 0.25-mm diameter propellant inlet was drilled in the center of the cathode and a second 0.5-mm hole was drilled off axis to allow pressure measurements in the discharge chamber. Opposite the cathode is a 1-mm diameter cylindrical, aluminum hollow anode. The flat inner surface of the electrode was covered with a 5 mil thick mica disk. To operate as a complete thruster the NMIMT would require extraction and accelerating grids and a plasma charge neutralizer. This initial investigation is interested in the ionization effectiveness of the discharge chamber only.

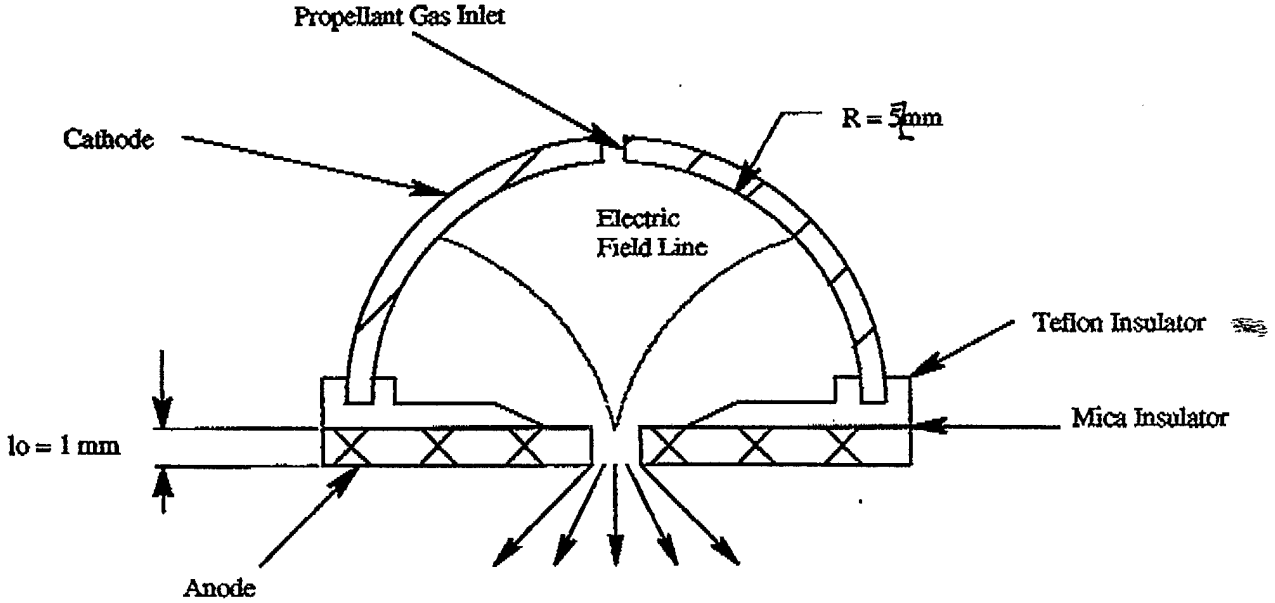


Fig. 2 NMIMT Discharge Chamber Schematic

## II. Theory

A simple model can be used to estimate the degree of ionization in the discharge chamber. The insulation on the inside surface of the outer electrode prohibits the electric field lines from attaching to the surface as shown in Fig.2. Therefore, the field lines only attach to the hollow anode surface which has a focusing effect on the electrons that are emitted from the cathode. The electrons arrive close to the anode

accelerated through a significant fraction of the acceleration voltage in the cathode fall region. In this region, they ionize the discharge gas which is flowing through the orifice into the vacuum chamber. The discharge gases are exposed to the intense electron current for some time $\tau$, the residence time in the orifice of length $l_o$ as given in Eq 6.

$$\tau = \frac{l_o}{u_f} \tag{6}$$

where $u_f$ is the velocity at which the neutrals are travelling through the exit orifice. For expansion into a high vacuum, $u_f$ will be approximately the speed of sound in the discharge chamber as given by

$$u_f \approx (\gamma \frac{k}{m_d} T_o)^{\frac{1}{2}} \tag{7}$$

The electron current in the orifice is taken as $I_d$ so that the current density is $I_d/A_o$. Due to the electrons, this ionization rate per unit volume, since $n_e u_e = (6.24 \times 10^{18})(I_d/A_o)$, is given by

$$\dot{N}_I \approx (6.24 \times 10^{18}) \left( \frac{I_d}{A_o} \right) \sigma_I n_d \tag{8}$$

where $n_e$ is the electron number density, $u_e$ is the electron velocity, $n_d$ is the number density in the exit orifice, $A_o$ is the cross-sectional area of the exit orifice, and $\sigma_I$ is the electron impact ionization cross-section for the propellant gas. The total accumulated degree of ionization in the gas, assuming the ionization to be relatively small, is given by

$$\dot{N}_I \tau \approx \frac{\left[ (6.24 \times 18^{18}) \left( \frac{I_d}{A_o} \right) \sigma_I n_d l_o \right]}{u_f} \tag{9}$$

Assuming that the ion and neutral gas are flowing at the same speed, $u_f$, the degree of ionization, $\alpha_I$, is given by

$$\alpha_I = \frac{\dot{N}_I \tau}{n_d} = \left[ (6.24 \times 10^{18}) \left( \frac{I_d}{A_o} \right) \sigma_I \left( \frac{l_o}{u_f} \right) \right] \tag{10}$$

A typical value for the current density in a discharge is 1 A/cm$^2$. The electron impact ionization cross-section for argon at an energy of 150 eV is $3 \times 10^{-16}$ cm$^2$. The orifice length is 1 mm and the discharge chamber temperature is assumed to be 300K. This provides a rough estimate of the degree of ionization for the discharge chamber of 0.6%. Xenon has an ionization cross-section of $6 \times 10^{-16}$ cm$^2$ and has a mass ratio to argon of 3.25 providing an ionization degree of approximately 2%. This does not agree with the previous spectroscopic results[10] which indicate much higher degrees of ionization.

## III. Experimental Setup

The test facility used in reviewing the discharge chamber was a 0.3m diameter stainless steel vacuum chamber. Vacuum pumping of the chamber was done by a rotary vane mechanical pump and an 800 l/s turbomolecular pump through a side mounted port. The system provided an ultimate pressure in the chamber of $1 \times 10^{-5}$ Torr. Fig. 3 shows the NMIMT discharge chamber ($p_{dc}$) and vacuum chamber ($p_{vac}$) pressures for various mass flows.

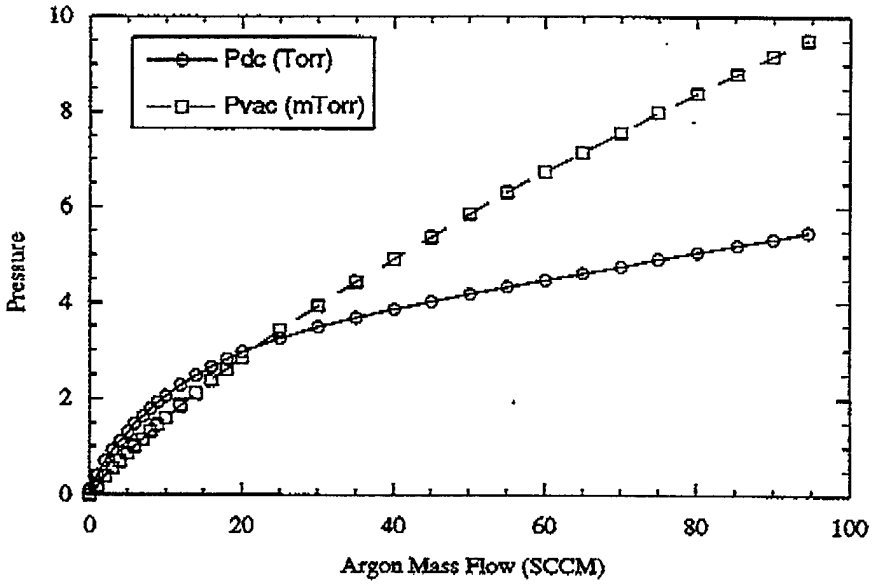


Fig. 3 NMIMT Discharge Chamber and Vacuum Chamber Pressure Relationships

Fig. 4 illustrates the optical and plasma probe diagnostic setup for the NMIMT discharge chamber. The thruster can be positioned in two locations to allow spectroscopic investigation of the light emitted axially and normally to the plume direction. The collected light is collimated and focussed on the entrance slit of a 0.85-m double spectrometer. The Langmuir probe is mounted 2.5 cm downstream from the exit orifice of the discharge chamber with the disk surface normal to the axis of the plume. The diameter of the probe is 5.5 mm, and it is mounted normal to the plume flow direction to operate as a stagnation type Langmuir probe. The current collected by the Langmuir probe is inferred by measuring the voltage drop across a 1 MΩ resistor.

The discharge was operated on argon to allow comparisons with previous studies[10] and to investigate the different modes of operation while avoiding the costs of running on xenon. A variable resistor was placed in the power line to aid in the starting of the discharge. The discharge is struck at a higher voltage than the minimum normal operating voltage at the given pressure. The resistor allows a high voltage to be initially applied to the discharge. As soon as the discharge is struck and current is drawn the voltage applied to the discharge is lowered to operational levels. The discharge could be operated at pressures above 0.75 Torr, with discharge currents up to 15 mA.

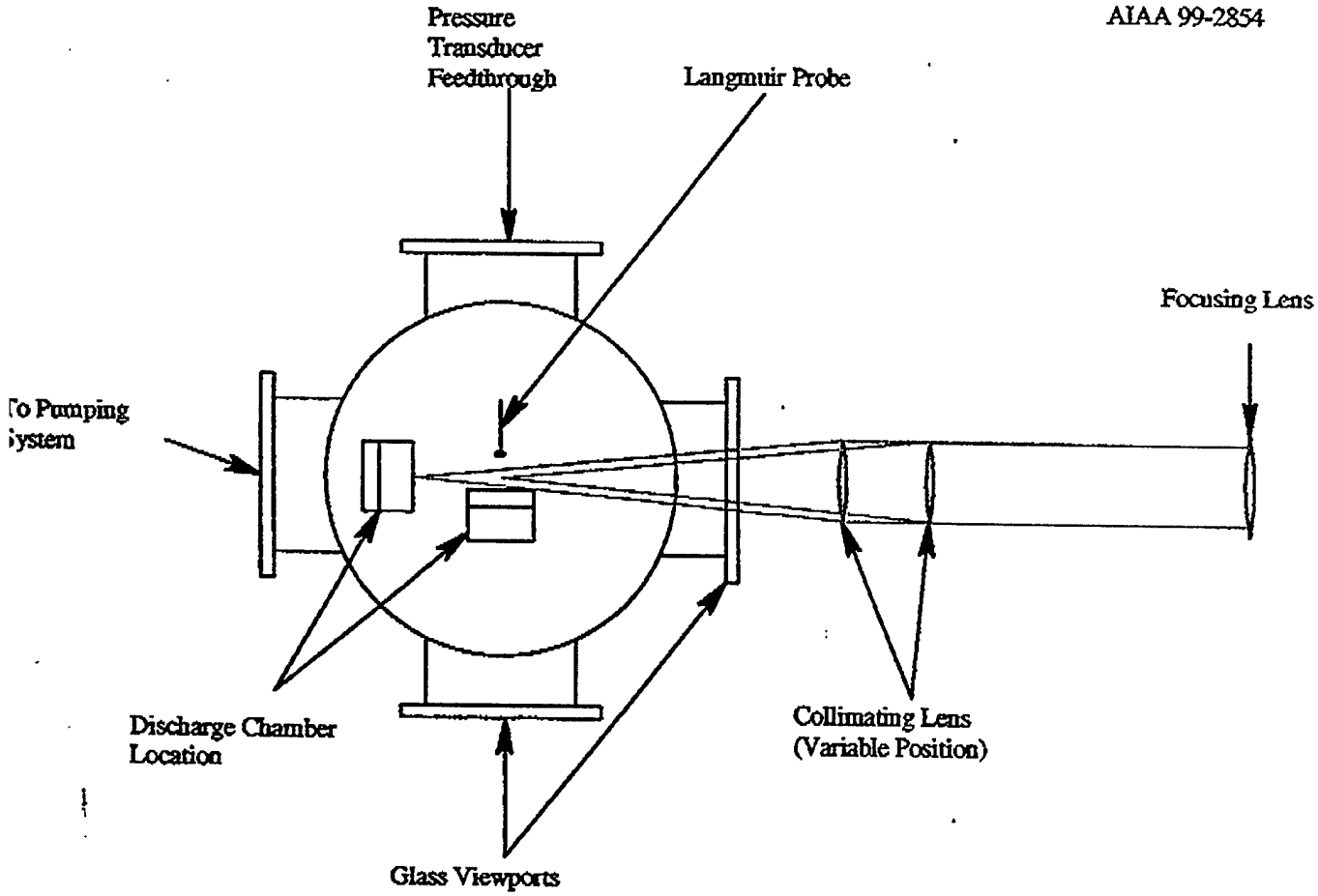


Fig. 4 Diagnostics Setup

## IV. Results

### A.) Operating characteristics

Fig. 5 shows the current verses voltage relationship for the discharge chamber at different operating pressures. It resembles a typical V-I characteristic for an abnormal glow discharge. Transitions to an undesired arc are not observed for discharge currents up to 10 mA. A light degradation of the hemispherical cathode was observed with it primarily located near the small entrance holes. No degradation was observed on the hollow anode surface.

glow?

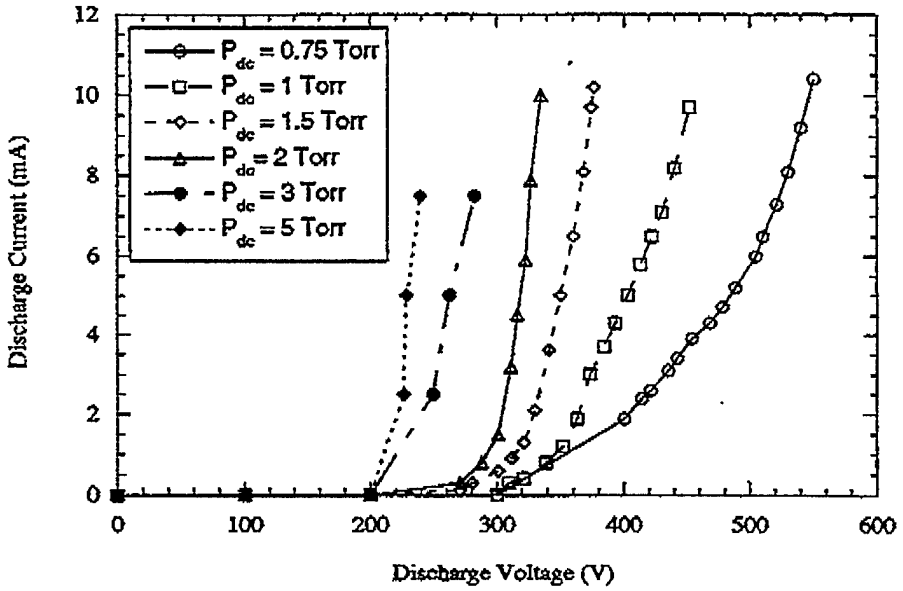


Fig. 5 V-I Characteristics of the NMIMT Discharge Chamber

**B.) Spectroscopy**

Two spectroscopic configurations were used to analyze the NMIMT discharge chamber plume. The first was to collect light axially along the plume axis with the collecting lens focused on the exit orifice (hollow anode). This method is very qualitative in nature because it integrates along the axis collecting information about the discharge from the exit orifice through the end of the plume. This method was used to compare with previous results[10] for a similar discharge chamber. The spectrometer used was a 0.75m double spectrometer. The slit widths were kept between 50 and 200 μm.

An attempt was made to run the discharge at the same conditions as during the previous studies,[10] but limited published information made the direct comparisons difficult. A wide variety of operating conditions were investigated and all of the resulting spectra contained neutral lines. Fig. 6 is a spectrum taken for a discharge current of 1.25 mA and a discharge pressure of 0.75 Torr. Fig. 6 shows the strong neutral lines that were present in the far red portion of the spectrum regardless of the operating conditions used in this research. Although the trend is to reduce the neutral to ion ratios as the discharge current increases, the neutral lines in the spectrum are always present. Fig. 7 shows neutral to ion line ratios for the discharge chamber plume at a discharge pressure of 1 Torr.

The other spectroscopic configuration collects light normal to the plume axis at a distance of 1cm downstream of the end of the exit orifice. This method was expected to gain relative information about the discharge chamber in different modes of operation; however it provided no information since ion lines were not detected in this mode.

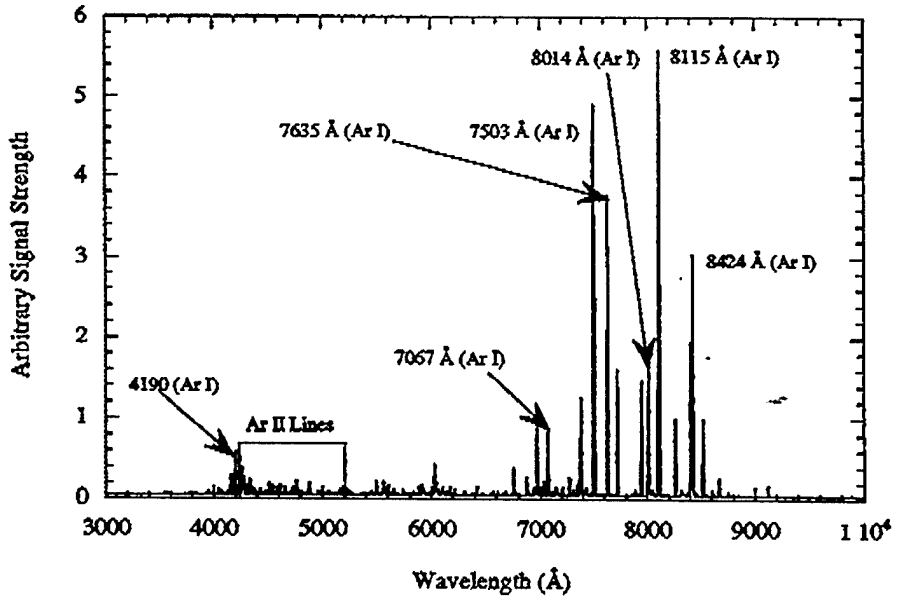


Fig. 6 Typical Spectrum of the NMIMT Discharge Chamber

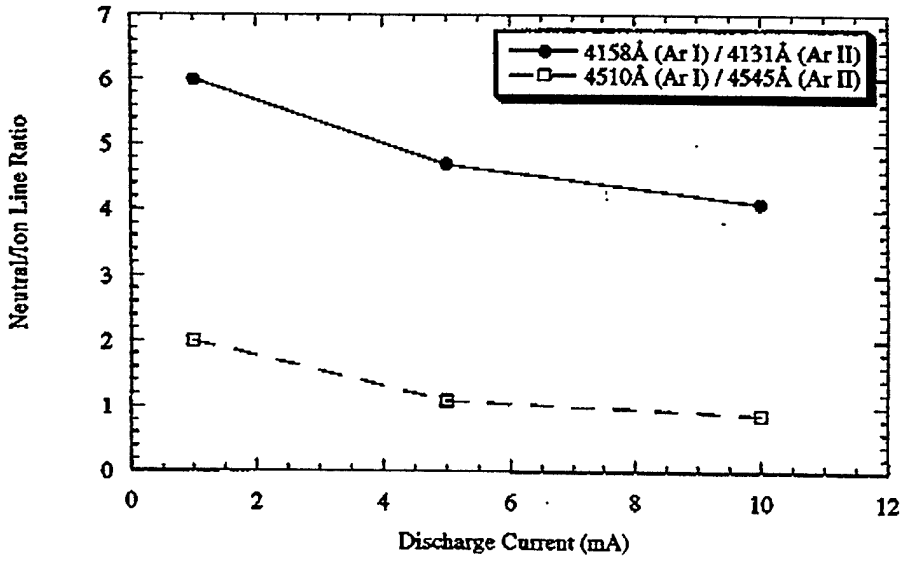


Fig. 7 Neutral to Ion Line Intensity Ratios at Different Discharge Conditions

### C.) Langmuir probe

Langmuir probes are common diagnostic tools used to study plasmas.[14] In the investigation of the initial discharge chamber chosen for the NMIMT a disk shaped Langmuir probe with a diameter 0.55 cm is used to measure the ion current at a distance of 2.5 cm downstream of the discharge chamber. The ion flux is estimated from Eq. 11 by assuming that the ion saturation current was that current collected by the probe at a bias of –180 V.

$$\phi_i = \frac{I_{sat,I}}{eA_p} \tag{11}$$

where $I_{sat,I}$ is the ion saturation current collected by the probe, e is the unit charge, and $A_p$ is the frontal surface area of the Langmuir probe. The probe is a stagnation point type Langmuir probe with its longitudinal axis normal to the discharge chamber plume. The mean free path at the probe location is between 60 mm and 12 mm for discharge chamber pressures of 1 and 5 Torr, respectively. The number density at the probe location is primarily due to the plume gas as determined by Eq. 12. The Debye length at this location in the plume is between 0.2 and 0.5 mm depending on the discharge conditions. The sheath thickness around the probe is roughly four times the Debye length; therefore the probe sheath is slightly smaller than the diameter of the probe. This will cause the results obtained by using the planar probe analysis to be only approximate, which is sufficient for the first analysis of the discharge chamber.

By comparing the ion flux to the expected neutral flux at this distance, the degree of ionization can be estimated. Plume expansion into a perfect vacuum will provide an axial number density distribution given by[12]

$$n_n = n_d c_j(\gamma)\left(\frac{D_o}{r}\right)^2 \tag{12}$$

where $n_n$ is the neutral number density along the centerline of the plume at a distance r, away from an orifice of diameter $D_o$. $C_j$ is a factor that only depends on the specific heat ratio and is 0.15 for argon. If the neutrals are assumed to be sonic at the exit orifice, the velocity of the neutrals is given by

$$V_{j\max} = \left(\left(\frac{2\gamma}{\gamma-1}\right)\frac{kT_d}{m_d}\right)^{\frac{1}{2}}. \tag{13}$$

Since the flow is hypersonic and nearly free molecular at the probe position, the neutral flux will then be given by

$$\phi_n = n_n V_{j\max}. \tag{14}$$

The ionization degree is the ratio of the ion flux to the neutral flux ($\phi_i/\phi_n$). Fig. 8 shows the experimentally derived degree of ionization for the discharge chamber at different operating conditions.

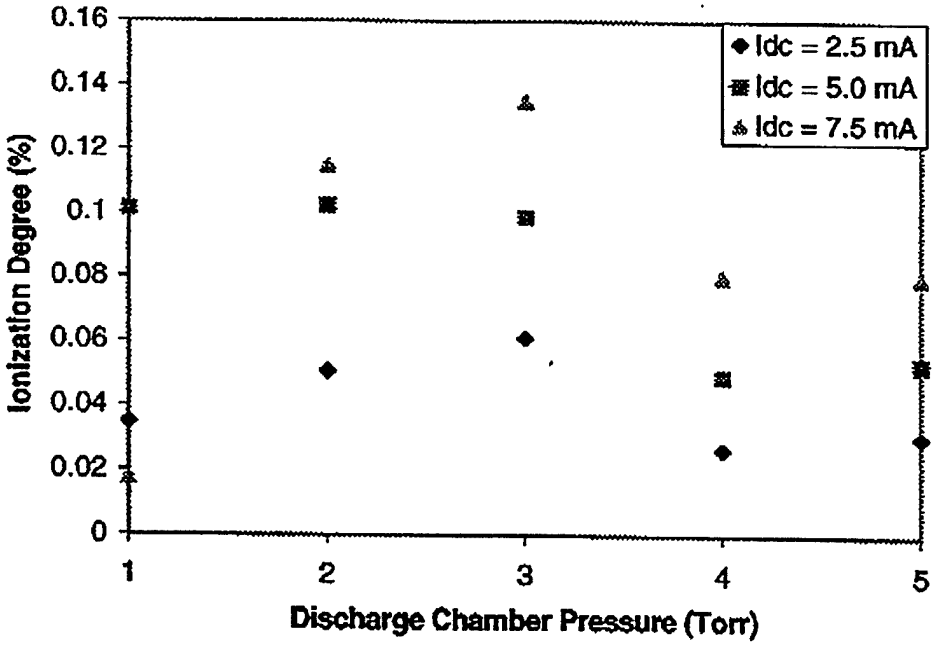


Fig. 8 NMIMT Discharge Chamber Efficiency

As shown in Fig. 8, the maximum ionization occurred for a discharge chamber pressure of 3 Torr for a given discharge current. The visible plume emanating from the hollow anode region of the discharge chamber almost disappeared when operating at discharge chamber pressure of 1 Torr and a discharge current of 7.5 mA. This condition was near the edge of the operational envelope of the discharge chamber as shown by the lower ionization degree than for the same current at higher pressures. The electron temperature can be estimated by plotting the natural log of $I - I_{sat,I}$ verses the probe potential. $I_{sat,I}$ is the ion saturation current. The slope of the line is $e/kT_e$, and from this the electron temperature, $T_e$, can be calculated. Fig 9 shows the estimated electron temperature at different discharge conditions. The electron temperature is quite high when compared to typical glow discharges. This is due to the hollow anode effect in the exit orifice[4,5,10], where electrons ballistically separate from field lines and emerge as an electron beam with an energy close to the cathode fall.

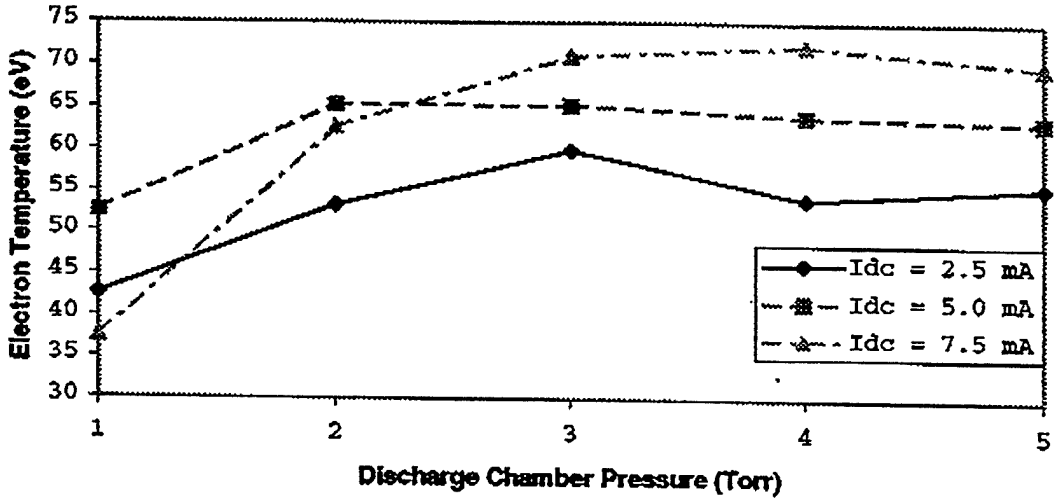


Fig. 9 NMIMT Plume Electron Temperature

An ion extraction ring was placed near the exit of the hollow anode. The ring has a diameter of 2 cm and was placed 1 cm downstream from the exit orifice. Fig. 10 illustrates the effect of the extraction ring on the current collected by the Langmuir probe at a discharge chamber pressure of 5 Torr. With a constant mass flow, the increased probe current relates directly to the degree of ionization in the plume. Fig. 10 shows the normalized probe current verses the extraction ring potential where $I_o$ is the current collected by the probe with zero bias on the ring.

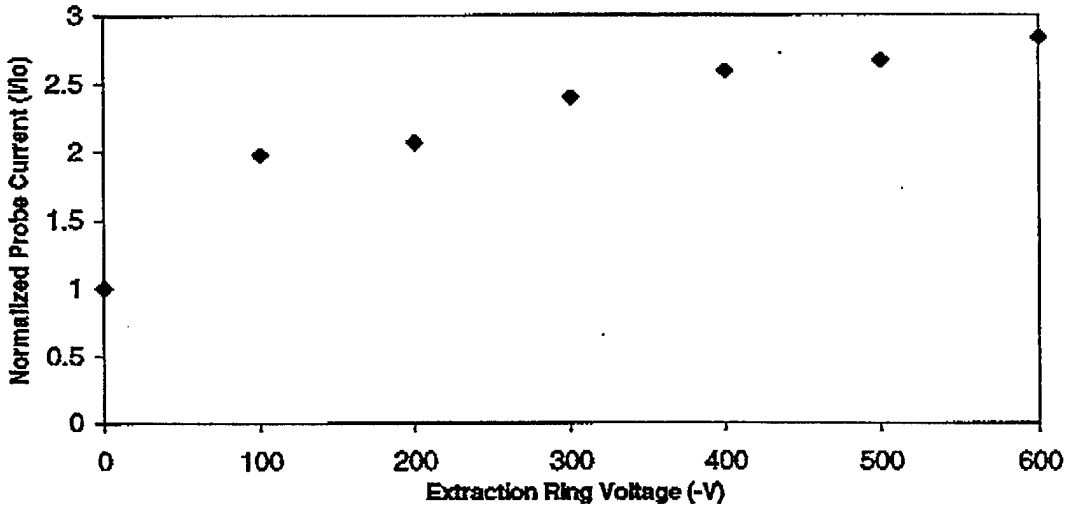


Fig. 10 Extraction Ring Effect on Discharge Chamber Plume

## V. Conclusions

The initial discharge chamber chosen for the NMIMT is shown to provide a lower degree of ionization than previous spectroscopic results indicated. A simple model predicts that the degree of ionization produced by the discharge chamber while running on argon is 0.6%. Attempts to reproduce earlier results failed, possibly due to insufficient published data on precise operating conditions. Langmuir probe measurements indicate that the discharge chamber provided a degree of ionization under 0.15%. The simple model is expected to overestimate the degree of ionization provided by the discharge chamber because it does not take into account the losses of ions and electrons to the walls. Spectroscopic studies found very strong neutral lines in the exhaust plume of the discharge chamber, which is contrary to the results of Miljevic. A simple extraction device was added to increase the degree of ionization in the exhaust plume. The extraction ring was able to provide roughly 3 times the plume ionization compared to the unextracted case. Further work is required to investigate potential schemes to increase the ionization degree.

## References

1. Yashko, G., Giffin, G., Hastings, D., "Design Considerations for Ion Microthrusters," IEPC 97-072, August 1997.

2. Mixon, P. D., Griffin, S. T., Williams, J. C., "Breakdown Voltage Scaling Characteristics of an Argon Hollow Cathode Discharge," Applied Spectroscopy, 47, 10, pp 1567-1570, 1993.

3. Filliben, Jeff D., "Electric Propulsion for Spacecraft Applications," CPTR 96-64, December 1996.

4. Allen, W.D., Hale, D.P., "Energy Distribution of Fast Electrons Present in Beams from Hollow Anode Gas Discharge Electron Guns," J. Phys., 3, pp 1912-1918, 1970.

5. Dugdale, R.A., "The Application of the Glow Discharge to Material Processing," J. Material Science, 1, pp 160-169, 1966.

6. Zhang, Z., Perry, N., Tobin, T., "Magnetic Field Enhanced Performance of a Copper Hollow Anode Cathode Laser," J. Appl. Phys., 71, 11, pp 5338-5343, 1992.

7. Pham-Van-Diep, G., Weaver, D.P., Dewitt, D., Trelles, J., Randolph, T., Muntz, E.P., "Properties of an Energetic O Atom Stream from a Gas Discharge Source," AIAA paper 90-1560, 1990.

8. Ketsdever, A.D., Muntz, E.P., Weaver, D.P., "A Facility to Produce an Energetic, Ground State Atomic Oxygen Beam for the Simulation of the Low Earth Orbit Environment," NASA Conference Publication 3280, pp 121, 1994.

9. Ketsdever, A.D., "The Production of Energetic Atomic Beams via Charge Exchange for the Simulation of the Low-Earth Orbit Environment," Ph.D. Thesis, University of Southern California, August 1995.

10. Miljevic, V.I., "Spectroscopy of hollow anode discharge," Applied Optics, 23, 10, pp 1598-1600, 15 May 1984.

11. Miljevic, V., "Hollow anode ion-electron source," Rev. Sci. Instrum., 55, 6, pp 931-933, 1984.

12. Miljevic, V.I., "Characteristics of the hollow anode ion-electron source," IEEE Transactions on Nuclear Science, NS-32, 5, pp 137-138, October 1985.

13. Miljevic, Vujo I., "Optical characteristics of the hollow anode discharge," J. Appl. Phys. 59, 2, pp 676-678, 22 July 1985.

14. Swift, J.D., Schwar, M.J.R. (1969) *Electrical Probes for Plasma Diagnostics*, American Elsevier: New York.

15. Ashkenes, H., Sherman, F.S., "Structure and utilization of supersonic free jets in low density wind tunnels," In: de Leeuws J Ed. Rarefied Gas Dynamics. 84-98 New York: Academic Press, 1966.